inorganics

Article

Bi_2O_3-Modified Ceramics Based on $BaTiO_3$ Powder Synthesized in Water Vapor

Anastasia Kholodkova [1,2,*], Aleksey Smirnov [2], Marina Danchevskaya [1,2], Yurii Ivakin [1], Galina Muravieva [1], Sergey Ponomarev[2], Alexandr Fionov [3] and Vladimir Kolesov [3]

1 Chemistry Department, Lomonosov Moscow State University, 119991 Moscow, Russia; mn.danchevskaya@yandex.ru (M.D.); ivakin@kge.msu.ru (Y.I.); yelmaleaf@gmail.com (G.M.)
2 Center for Collective Use "Science-intensive technologies in machine engineering", Moscow State Polytechnic University, 115280 Moscow, Russia; alex-smv99@yandex.ru (A.S.); psgpsg1@yandex.ru (S.P.)
3 Kotel'nikov Institute of Radio-Engineering and Electronics of RAS, 125009 Moscow, Russia; fionov@cplire.ru (A.F.); kvv@cplire.ru (V.K.)
* Correspondence: anastasia.kholodkova@gmail.com; Tel.: +7-495-939-4753

Received: 30 November 2019; Accepted: 21 January 2020; Published: 23 January 2020

Abstract: Bi_2O_3 was investigated in the role of a modifier for $BaTiO_3$ powder synthesized in a water vapor atmosphere at 200 °C and 1.55 MPa. Modification was aimed at increasing the sinterability of the powder as well as improving the structural and dielectric properties of the obtained ceramics. The morphology and phase contents of the synthesized $BaTiO_3$ powder were controlled by the methods of SEM and XRD. Properties of pure and Bi-doped $BaTiO_3$ ceramics were comprehensively studied by XRD, SEM, dielectric spectroscopy, and standard approaches for density and mechanical strength determination. Doping with Bi_2O_3 favored $BaTiO_3$ ceramic densification and strengthening. The room-temperature dielectric constant and the loss tangent of Bi-doped $BaTiO_3$ were shown to stabilize within the frequency range of 20 Hz to 2 MHz compared to non-doped material. The drop of dielectric constant between room temperature and Curie point was significantly reduced after Bi_2O_3 addition to $BaTiO_3$. Bi_2O_3 appeared to be an effective modifier for $BaTiO_3$ ceramics produced from non-stoichiometric powder synthesized in water vapor.

Keywords: barium titanate; water vapor; bismuth oxide; sintering additive; ceramics modification; densification; microstructure; dielectric constant; loss tangent

1. Introduction

Barium titanate $BaTiO_3$ is an important ferroelectric widely applied in the production of ceramic components for numerous microelectronic devices such as multilayer ceramic capacitors (MLCC), piezoelectric transducers, positive temperature coefficient resistors (PTCR), actuators, etc. [1–4]. The ferroelectric properties of $BaTiO_3$ originate from spontaneous polarization and appear in its crystals on cooling to a certain temperature (Curie temperature, T_{Curie} = 120–130 °C) corresponding to cubic to tetragonal phase transition. This kind of polarization in $BaTiO_3$ is caused by displacement of Ti^{4+} ions from the central positions of cubic unit cells during their transformation to tetragonal cells. These displacements occur unidirectionally within certain crystalline regions called ferroelectric domains. Neighboring domains compensate each other's polarizations owing to their different directions. When an electric field is applied, a spontaneous polarization vector follows the electric field vector in ferroelectric crystals [5]. The most attractive properties of $BaTiO_3$ are the low Curie temperature and high dielectric constant accompanied by relatively low loss tangent. $BaTiO_3$ ferroelectric phase transition corresponds to a rise of dielectric constant up to several thousands. This order of magnitude is maintained by the dielectric constant down to ambient temperature.

One of the main challenges of $BaTiO_3$ ceramics production is achieving high material density close to its theoretical value [6]. The density is determined by the microstructure of the ceramics. Structural inhomogeneity related to porosity as well as trace amounts of moisture which is inevitably closed into the pores cause the increase of ceramic conductivity and worsen its functional properties. Controlled dispersity of the starting $BaTiO_3$ powder and tuned technological parameters of ceramic manufacturing would allow obtaining dense material with low structure defectiveness as desired for MLCCs and other devices [7].

A known approach to modification of oxide ceramic properties is the use of different oxide additives [8–10]. Their incorporation into the initial lattice may affect the rates of sintering and grain growth or lead to liquid phase formation. Additives which form high-temperature melts provide wetting of the individual starting particles and formation of concave necks between them. Capillary forces pull the particles together, yielding in powder compaction. The melt facilitates mutual orientation of the particles, increases the contact area between them, and promotes shrinkage of the sample. Chemical interaction of the additive and the main component intensifies solid-state mobility in a compact and reduces the activation energy of volume and surface diffusion during the sintering. As a result, obtaining a material with increased density and strength is expected.

A method of $BaTiO_3$ synthesis in water vapor atmosphere was proposed in recent works [11–15]. In contrast to the traditional hydrothermal method which is usually based on a reaction between the species in a solution, this method of synthesis includes the treatment of an initially dry barium and titanium oxides mixture in water vapor in equilibrium with liquid. Having an advantage over the hydrothermal route, the synthesis in water vapor leads to lower water and hydroxyl group contents in the product and results in narrower $BaTiO_3$ crystal size distribution [13]. The method is ecologically benign owing to the mild conditions of the synthesis and high atomic efficiency. The obtained $BaTiO_3$ powder performed high sinterability under spark plasma sintering (SPS) conditions [14]. The corresponding ceramics possessed a homogenous microstructure, submicron grain size, and a dielectric constant of 1500–2300 at room temperature at 1 MHz. However, when sintered by the more available and widespread conventional route, ceramics based on $BaTiO_3$ synthesized in vapor conditions achieved lower density and had insufficient dielectric properties [12].

In the present work steps were taken to improve the microstructural and dielectric properties of these $BaTiO_3$ ceramics by modification of the initial powder composition. One of the typical modifications of $BaTiO_3$ ceramics is incorporation of Bi^{3+} ions [16–22]. As reported earlier, the use of Bi_2O_3 additive to $BaTiO_3$ powder promoted ceramic densification owing to liquid phase formation during the sintering [23–25]. Bi^{3+} ion is known to substitute aliovalently Ba^{2+} in a perovskite lattice because of similar ionic radii (0.145 and 0.160 nm, respectively) [18,23–27]. The solubility limit of Bi^{3+} in $BaTiO_3$ was reported to reach 5 at % [28]. The charge compensation mechanism leads to formation of barium vacancies which promote solid-state mobility and consequently decrease the energy required for sintering [18]. $BaTiO_3$ modification with Bi^{3+} ions is used industrially to lower its sintering temperature [18,19]. Besides, Bi-doping plays an important role in modification of the dielectric properties of $BaTiO_3$-based ceramics, for instance, in flattening of its dielectric response in a certain temperature range, and in turning its behavior to relaxor ferroelectric or n-type semiconducting [27,29–31]. Bi_2O_3 is often used in the production of complex oxide dielectric compositions such as solid solutions or layered structures with tuned dielectric characteristics [16].

Bi_2O_3 addition was expected to facilitate the sintering of $BaTiO_3$ powder synthesized in water vapor atmosphere, favor the formation of a homogenous microstructure, and raise its dielectric properties to the desired level.

2. Results

2.1. $BaTiO_3$ Powder Characterization

$BaTiO_3$ synthesis was carried out from a mixture of barium and titanium oxides which was treated in a water vapor atmosphere at a temperature of 200 °C and a corresponding autogenous pressure of 1.55 MPa for 20 h. The phase composition of the synthesized powder turned out to be sensitive to the molar ratio of initial oxides in the reaction mixture (Figure 1, Table 1). A significant amount of unreacted TiO_2 was found in a product synthesized from an equimolar mixture of BaO and TiO_2 (sample BT-100). Traces of rutile were also detected in powders produced with the use of excessive BaO amounts relatively to TiO_2 (Ba/Ti = 1.10 and 1.20, samples BT-110 and BT-120). Unreacted barium compounds were removed from the product by washing with acetic acid solution and distilled water. Single-phase $BaTiO_3$ was obtained from a mixture of simple oxides with Ba/Ti = 1.25 (sample BT-125). The detected peaks corresponded to cubic $BaTiO_3$ modification. Metastability of this phase (also called pseudocubic) below the temperature of phase transition to tetragonal modification (T_{Curie} = 120–130 °C) could be explained by the influence of the remaining structural hydroxyl groups and charged defects which deteriorated the spontaneous polarization [32]. A detailed examination of the background found no minor phases in the sample BT-125 (Figure 1, inset). Incomplete transformation of the reagents observed when lower BaO excess was used can be attributed to the diffusion factor governing $BaTiO_3$ formation in water vapor conditions. Single-phase $BaTiO_3$ powder is preferable for subsequent ceramic processing [7]. The sample BT-125 was subsequently used in ceramic manufacturing.

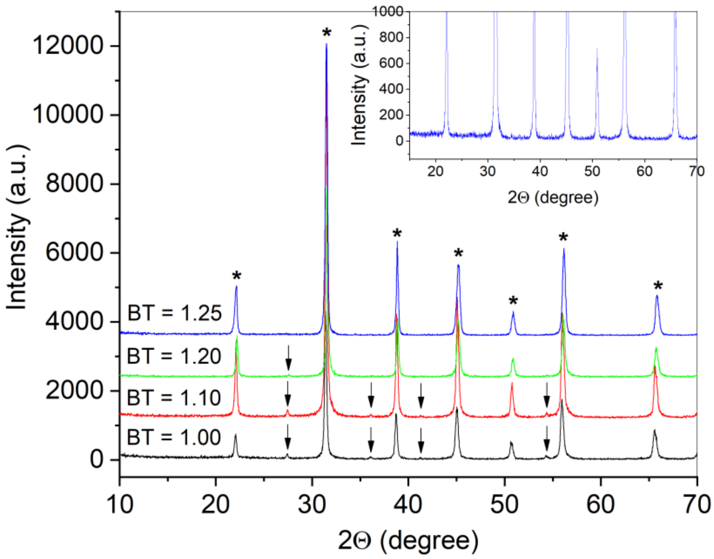

Figure 1. XRD patterns of $BaTiO_3$ powders synthesized at 200 °C, 1.55 MPa over 20 h. in water vapor with the use of different Ba/Ti molar ratio (BT) in the reaction mixture (indicated). The powders were washed with acetic acid solution and distilled water after the synthesis. * asterisk indicated peaks correspond to $BaTiO_3$ (PDF-2 No. 00-031-0174), arrow indicated peaks correspond to TiO_2 (rutile, PDF-2 No. 00-021-1276).

Table 1. Ba/Ti molar ratio in the reaction mixture and phase composition of the synthesized powders after Ba^{2+} excess removal.

Sample	Initial Ba/Ti Molar Ratio	Mass Fractions in the Product (%)	
		$BaTiO_3$	TiO_2
BT-100	1.00	92.7	7.3
BT-110	1.10	96.0	4.0
BT-120	1.20	98.4	1.6
BT-125	1.25	100.0	0.0

XRF analysis of the single-phase $BaTiO_3$ powder (sample BT-125) revealed barium ion deficiency towards stoichiometry (determined ratio Ba/Ti = 0.82). This effect was explained by the particular leaching of Ba^{2+} ions from the surface of the powder while being washed in acid solution after the synthesis [14]. Barium leaching has often been observed in $BaTiO_3$ particles synthesized in solution by hydrothermal or related techniques because of high defectiveness and chemical activity of their surface [33–35].

Figure 2 shows the morphology and particle size distribution of the sample BT-125. The powder consisted of agglomerated round-shaped particles with a total mean size of 110 nm.

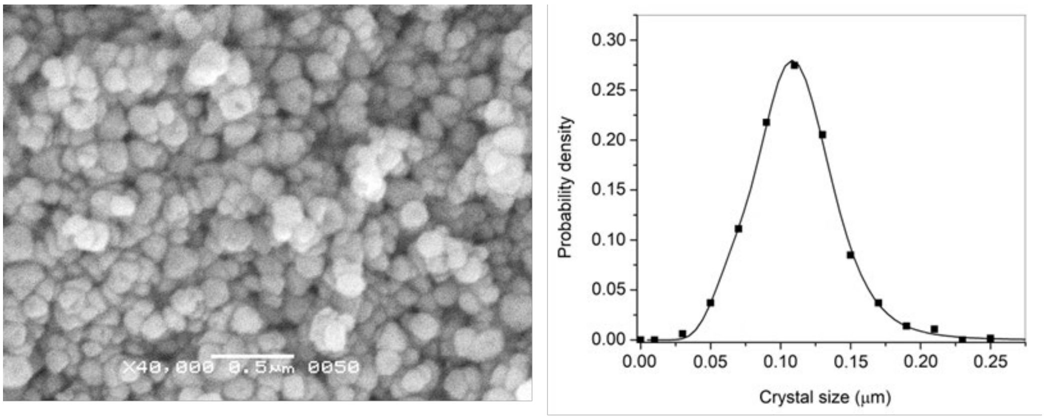

(a) (b)

Figure 2. SEM image (**a**) and particle size distribution (**b**) of $BaTiO_3$ powder synthesized at 200 °C, 1.55 MPa over 20 h. in water vapor.

2.2. Phase Composition of Bi_2O_3-Modified $BaTiO_3$ Ceramics

XRD patterns of pure and Bi-doped barium titanate ceramics are shown in Figure 3. The main component of the prepared ceramic samples was tetragonal $BaTiO_3$ (Figure 3). Along with this phase, X-ray patterns contained minor peaks of barium polytitanates, i.e., $BaTi_2O_5$ and $BaTi_4O_9$. Secondary phases found in the non-modified $BaTiO_3$ ceramics as well as in the samples with comparatively low addition of Bi_2O_3 (up to 0.5 mol %) could be explained by the non-stoichiometry of the starting powder. The lack of A-site ions in perovskite ABO_3 structure of the synthesized powder caused formation of Ti-rich phases during the sintering. However, the increase in Bi_2O_3 initial amount to 2.5–5.0 mol % was accompanied by smoothing of minor phase peaks which pointed to lowering of their contents (Figure 3a). This can be attributed to partial occupation of vacant A-positions in perovskite by Bi^{3+} ions. Barium substitution by bismuth easily occurred in the studied conditions owing to the $BaTiO_3$ initial non-stoichiometry.

The changes in phase composition of ceramics at a fixed level of doping (0.5 mol % Bi_2O_3) and varied sintering temperature are presented in Figure 3b. Raising of the sintering temperature led to disappearance of some secondary phase peaks. However, traces of $BaTi_2O_5$ were detected in the sample sintered at 1250 °C (Figure 3b).

The changes of $BaTiO_3$ unit cell parameters with the increase in Bi-doping resulted in a complicated character which originated from the initial non-stoichiometry of the perovskite-type oxide (Figure 4). In non-doped $BaTiO_3$, the presence of negatively charged Ba^{2+}-vacancies was presumed to be compensated by the positive charge of oxygen vacancies. This type of defectiveness can lead to the shrinkage of the unit cell in comparison to "ideal" $BaTiO_3$ crystal. Incorporation of Bi^{3+} ions into vacant Ba^{2+} positions and simultaneous elimination of oxygen vacancies, which occurred according to the equation (follows Kroger–Vink notation): $Bi_2O_3 \rightarrow 2\ Bi_{Ba}^{\bullet} + V_{Ba}'' + 3\ O_O^{\times}$, resulted in a notable increase in both *a* and *c* parameters of the $BaTiO_3$ tetragonal cell. This was notably manifested in the case of 0.1 mol% Bi_2O_3 addition and was also accompanied by a leap of tetragonality *c*/*a*. Besides barium vacancy occupation, Bi^{3+} ions promoted further elongation of the *c* parameter of $BaTiO_3$ cell because of the polarization effect of its lone electron pair on the off-centered Ti^{4+} ion [20]. Doping with higher amounts of Bi_2O_3 maintained a certain concentration of barium vacancies while oxygen vacancy concentration was expected to decrement gradually. The observed dependence of $BaTiO_3$ lattice parameters and tetragonality on Bi_2O_3 content exceeding 0.5 mol % was in line with the data reported earlier for stoichiometric Bi-doped $BaTiO_3$ ceramics [20].

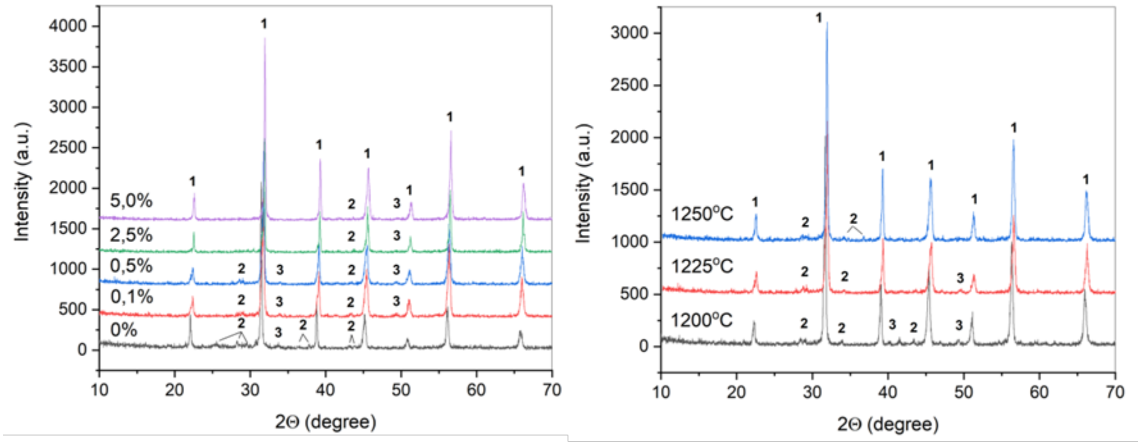

(a) (b)

Figure 3. XRD patterns of $BaTiO_3$ ceramics prepared with Bi_2O_3 addition: (**a**) sintered at 1225 °C with different amounts of Bi_2O_3; (**b**) sintered at different temperature with 0.5 mol % Bi_2O_3. Numbers indicated the following phases from PDF-2 database: 1—$BaTiO_3$ (PDF-2 No. 00-074-1956); 2—$BaTi_2O_5$ (PDF-2 No. 00-070-1188); 3—$BaTi_4O_9$ (PDF-2 No. 00-077-1565).

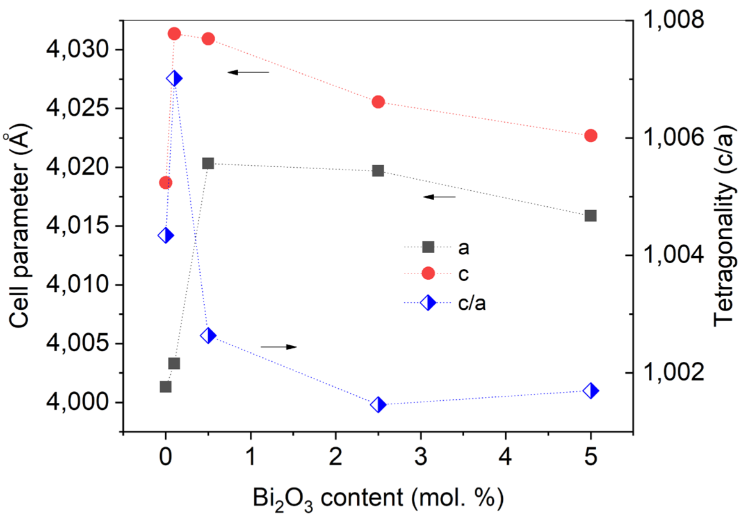

Figure 4. Cell parameters and tetragonality of $BaTiO_3$ ceramics sintered at 1225 °C with Bi_2O_3 addition.

EDX mapping of a fracture surface of $BaTiO_3$ ceramics doped with 5.0 mol % Bi_2O_3 revealed homogenous distribution of all contained elements including bismuth (Figure 5). Bismuth ions appeared to substitute barium in its positions uniformly over the whole grains of $BaTiO_3$. This kind of Bi^{3+} distribution was reported for $BaTiO_3$-based ceramics with a comparable doping level [36,37].

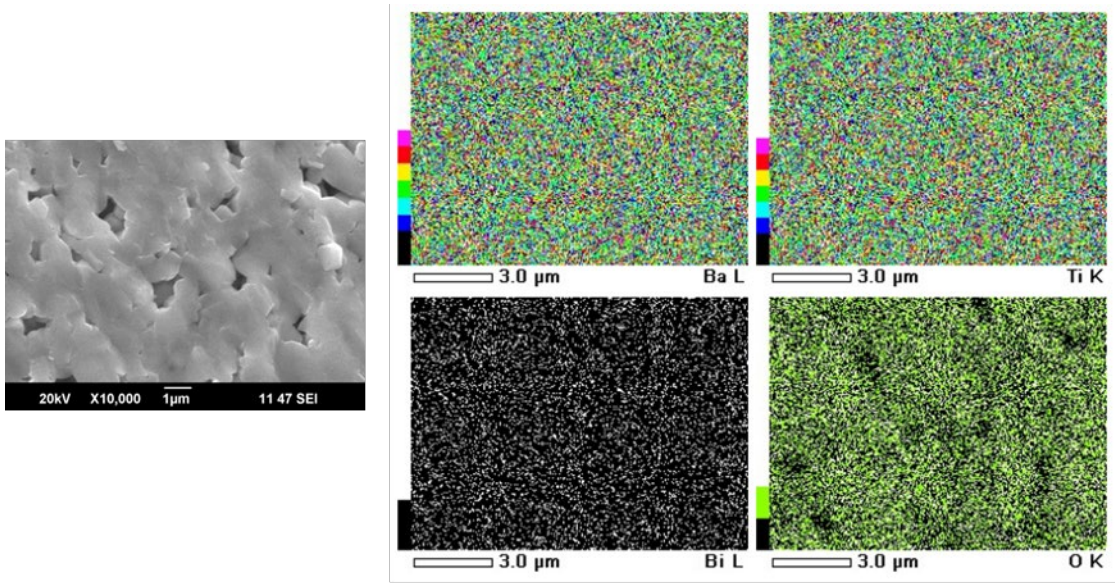

(a) (b)

Figure 5. SEM image (**a**) of fractured $BaTiO_3$ ceramics doped with 5.0 mol % Bi_2O_3 and its EDX mapping images (**b**) for the following elements: Ba, Ti, Bi, and O.

2.3. Structural and Mechanical Properties of Bi_2O_3-Modified $BaTiO_3$ Ceramics

Figure 6a shows the effect of the Bi_2O_3 additive amount on $BaTiO_3$ ceramic density. In the series of ceramic samples sintered at 1200 and 1225 °C, the relative density passed through a maximum with increasing Bi_2O_3 content. After the sintering at 1200 °C, the highest density of 4.88 g cm^{-3} was achieved at 2.5 mol % Bi_2O_3. Sintered at 1225 °C, the ceramics performed the highest densification up to 5.17 g cm^{-3} when doped with 0.1 mol % Bi_2O_3. When modified with 5.0 mol % Bi_2O_3, these ceramics possessed a density comparable to non-doped material. At a higher sintering temperature (1250 °C), the rise of the additive content was accompanied by a monotonic decrease in the density of the ceramics which pointed to an overheating phenomenon. Interestingly, this temperature appeared too low for the sintering of non-doped ceramics. Currently, the relative density of pure $BaTiO_3$ ceramics prepared at 1250 °C has reached only 76.3%. However, previously sintered at 1300 °C, it resulted in a density of 86.0% of theoretical [12]. The highest density among the studied samples reached 86.2% of its theoretical value and was obtained by ceramics sintered at 1225 °C with addition of 0.1 mol % Bi_2O_3. Passing through a maximum density with increasing bismuth content appeared to be typical for doped $BaTiO_3$ ceramics [23,25]. The currently observed result was comparable to densification of Bi-doped $BaTiO_3$ synthesized by a solid-state method with barium deficiency and sintered in a similar regimen [25].

A pronounced increase in the compressive strength of $BaTiO_3$ ceramics corresponded to low amounts of Bi_2O_3 additive (Figure 6b). The highest tensile strength after the sintering at 1200 °C was observed when the content of Bi_2O_3 was 0.5 mol %. Sintering at 1225 and 1250 °C resulted in ceramics with the highest strength in the case of 0.1 mol % Bi_2O_3. Addition of 0.1 mol % Bi_2O_3 improved the compressive strength of the ceramics after sintering at 1225 °C to 437 MPa compared to 140 MPa for pure $BaTiO_3$ ceramics manufactured with the same conditions. An increase in Bi_2O_3 content resulted in no further improvement in the strength characteristics of the material compared to pure $BaTiO_3$ ceramics.

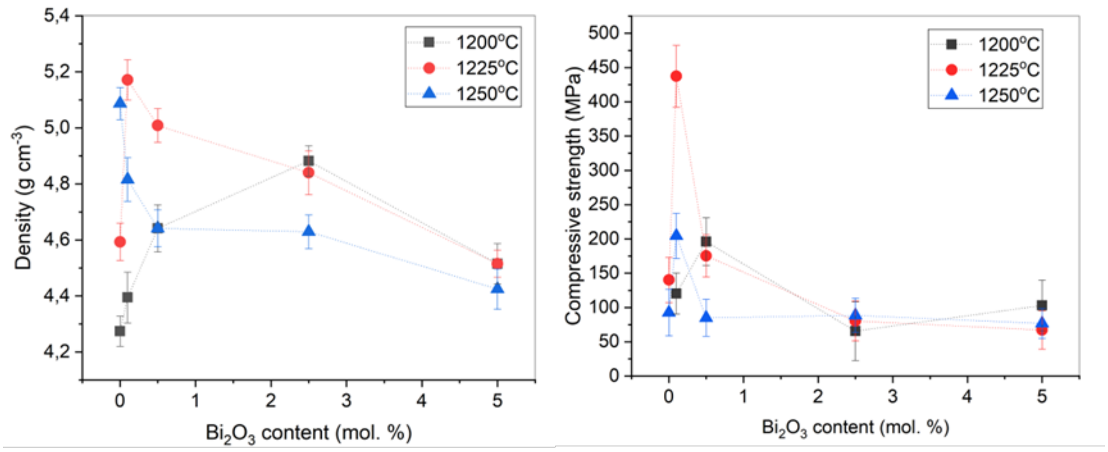

Figure 6. Relative density (**a**) and compressive strength (**b**) of $BaTiO_3$ ceramics sintered at 1200–1250 °C with different contents of Bi_2O_3 additive.

Electronic Industries Alliance (EIA) standards for capacitors widely applied by the manufacturers avoid regulation of the mechanical characteristics of the ceramic dielectric layer contained in the device. However, the mechanical strength as well as the dielectric strength are important indicators of capacitor ceramics reliability. Both these properties are very sensitive to the materials' microstructure and change jointly [38,39]. Hence, the value of the mechanical strength can be used as an indirect measure of the dielectric strength of a material.

Figure 7 shows the microstructure of $BaTiO_3$ ceramic samples modified with 0.1–0.5 mol % Bi_2O_3 and resulted in the highest relative density along with a microstructure of pure $BaTiO_3$ ceramics prepared with the same conditions (sintered at 1225 °C for 1 h.). Images of fracture and the surface of pure $BaTiO_3$ ceramics revealed considerable porosity in agreement with the density measurements (Figure 7a,d). The reduction of pore space was revealed as an effect of Bi_2O_3 addition and was accompanied by an increase in the density of the samples compared to non-doped material. The pores visible in the fractured ceramics containing 0.1 mol % Bi_2O_3 (Figure 7b) were more numerous than in the sample sintered with 0.5 mol % Bi_2O_3 (Figure 7c), and more evenly distributed. The surface image of the latter (Figure 7f) revealed small submicron pores neighbored by larger micron-sized ones and voids forming owing to pore coalescence. The sample with 0.1 mol % Bi_2O_3 was shown to have higher density (Figure 6a). Different character of pore size distribution in the considered samples could affect their mechanical properties in addition to porosity value. Among the parameters determining the strength of a ceramic material, an important role belongs not only to the total value of the porosity but also to the pore–stress interactions determined by the number and the size of pores as well as by the thickness of struts between them [40]. The higher compressive strength achieved by the $BaTiO_3$ sample modified with 0.1 mol % Bi_2O_3 compared to other samples sintered at 1225 °C could be attributed both to its higher density and uniformity of pore structure.

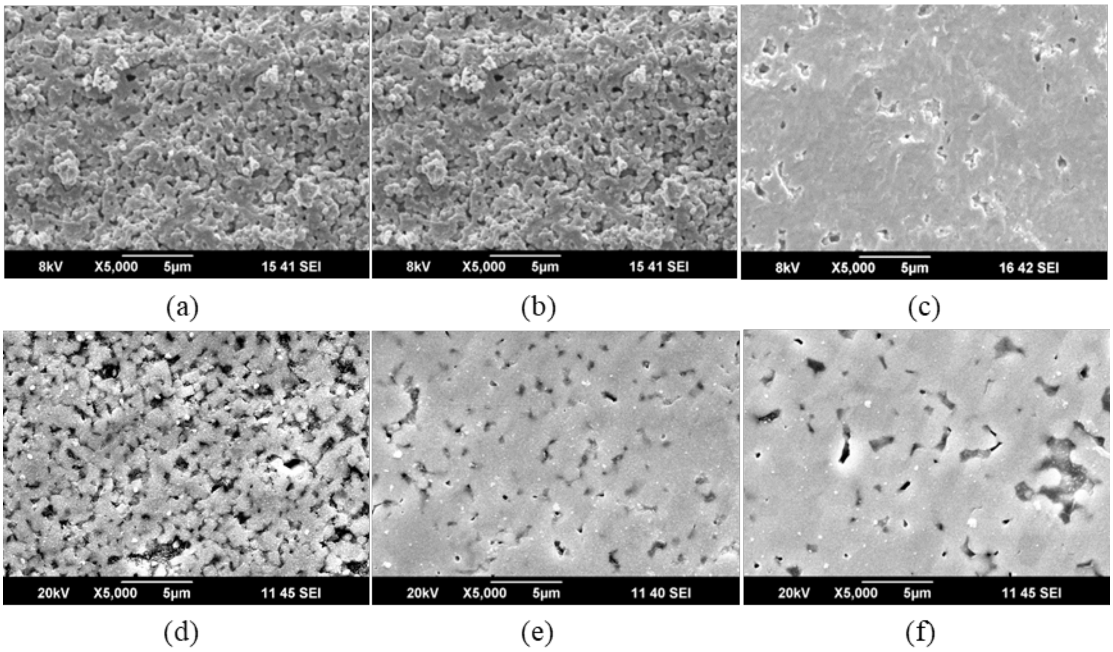

Figure 7. SEM images of fractured $BaTiO_3$ ceramics (**a**–**c**) and their polished surfaces (**d**–**f**) after the sintering at 1225 °C: (**a**) and (**d**)—without Bi_2O_3 addition; (**b**) and (**e**)—modified with 0.1 mol % Bi_2O_3; (**c**) and (**f**)—modified with 0.5 mol % Bi_2O_3.

2.4. Dielectric Properties of Bi_2O_3-Modified $BaTiO_3$ Ceramics

The dielectric properties of pure and Bi_2O_3-modified $BaTiO_3$ ceramics sintered at 1225 °C are shown in Figure 8. Non-doped ceramics achieved relatively poor dielectric characteristics revealing high sensitivity of the dielectric constant and the loss tangent to the frequency. A-site deficiency and phase inhomogeneity of this sample caused increased concentration of charged defects which resulted in high dielectric losses at low frequencies [41]. Compared to the pure $BaTiO_3$, ceramics prepared with the addition of Bi_2O_3 achieved more stable values of the dielectric constant and loss tangent within the frequency range of 20 Hz to 2 MHz. The highest room-temperature dielectric constant among the Bi-containing ceramics reached 1310 and was obtained by the sample with addition of 0.1 mol % Bi_2O_3. Also, this sample was characterized by low loss tangent (0.025–0.038) which slightly varied in the studied frequency range compared to pure $BaTiO_3$. Ceramics doped with 0.1–0.5 mol % Bi_2O_3 achieved a higher dielectric constant than the non-doped sample in the range of 1–2 MHz.

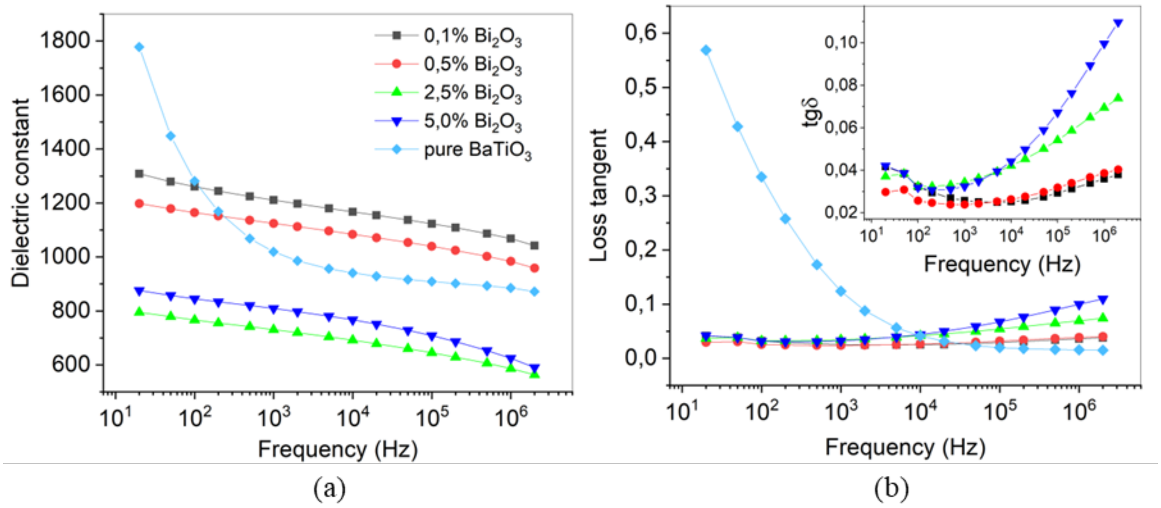

Figure 8. Dielectric constant (**a**) and loss tangent (**b**) vs. frequency for $BaTiO_3$ ceramics sintered at 1225 °C with different contents of Bi_2O_3.

Figure 9 shows the dielectric properties of ceramic samples which possessed the highest density and compressive strength, i.e., a pure $BaTiO_3$ sample sintered at 1250 °C and two samples sintered at 1225 °C with addition of 0.1–0.5 mol % Bi_2O_3. The highest dielectric constant coupled with the low loss tangent was achieved by the ceramics modified with 0.1 mol % Bi_2O_3.

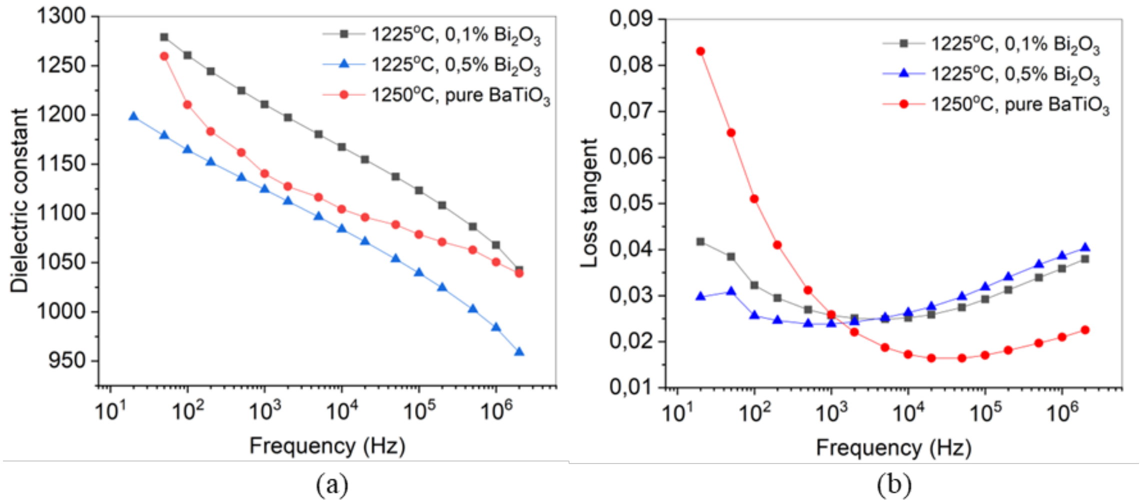

Figure 9. Dielectric constant (**a**) and loss tangent (**b**) vs. frequency for $BaTiO_3$ ceramics sintered under different conditions.

Pure $BaTiO_3$ ceramics sintered at 1250 °C underwent a ferroelectric phase transition at 121 °C (Table 2). The transition was accompanied by an increase in dielectric constant up to 3253 at 1 kHz. Bi^{3+} incorporation into the $BaTiO_3$ structure led to a slight shift of the phase transition point towards higher temperature and to lowering of ε_{max} value. This effect in aliovalently doped perovskite ferroelectrics was usually considered as a diffuse phase transition [23,25,27,41–43]. Bi^{3+} ions are known to induce a local electrical field in the volume of $BaTiO_3$ which interacts with the ferroelectric unit cell field and causes dispersion of the phase transition temperature over the sample [23,25,27]. The data reported on Bi^{3+} influence on ferroelectric phase transition in $BaTiO_3$-based ceramics appeared to be quite contradictory. Some of the authors noted no diffuse character of the transition for the materials with bismuth content within its solubility limit [26]. However, in other works the diffused behavior even on changing to relaxor type was observed [23,25,27]. Shift of the Curie point and lowering of the corresponding dielectric constant discovered in the current work proved the diffuse nature of the tetragonal to cubic phase transition in $BaTiO_3$ ceramics with addition of Bi_2O_3. It is practically beneficial leading to a diminished drop of dielectric constant within the working temperature range with the broadening of this range towards higher values.

Table 2. Dielectric constant at room temperature (ε_{RT}) and its maximum value (ε_{max}) at Curie temperature (T_C) measured at 1 kHz for $BaTiO_3$ ceramics with different Bi_2O_3 contents.

Bi_2O_3 Content (mol %)	Sintering Temperature	ε_{RT}	T_C (°C)	ε_{max}
0	1250	1127	121	3253
0.1	1225	1210	127	2540
0.5	1225	1124	133	2292

3. Discussion

This work provided novel results on the structural and dielectric properties of Bi-doped $BaTiO_3$ ceramics sintered from Ba-deficient powder synthesized in mild conditions of water vapor medium. Previously, non-stoichiometry of the powder was assumed to promote the growth of plate-like abnormal grains in ceramics [44] which led to a non-uniform microstructure and deteriorated the dielectric properties [12]. Currently, Ba^{2+} deficit in the synthesized $BaTiO_3$ powder caused secondary polytitanate phase formation during the sintering and increased conductivity which manifested itself in a pronounced frequency dependence of the room-temperature dielectric constant and loss tangent of the ceramics. Addition of Bi^{3+} ions to non-stoichiometric $BaTiO_3$ powder allowed slight lowering of the sintering temperature, improvement of the microstructure, achievement of higher phase homogeneity, and stabilization of the dielectric properties of the produced ceramics.

Bismuth oxide is well known as a sintering additive, which helps to increase the density and lower the sintering temperature of various oxide materials. However, in the present work, the introduction of Bi^{3+} ions did not always contribute to high densification of the material. The maximum density of the ceramics at a certain Bi^{3+} content and its further decrease with increasing doping level were found to be a common pattern at each of the applied sintering temperatures. The position of the maximum density shifted toward higher Bi^{3+} concentrations with decreasing sintering temperature. Apparently, an increase in Bi^{3+} content within the range of its solubility resulted in a continuous decrease in the optimum sintering temperature of the $BaTiO_3$ ceramics. The samples doped with 0.1 and 0.5% bismuth at 1225 °C as well as the non-doped sample prepared at 1250 °C were believed to be sintered at temperatures close to optimal for their compositions.

Another purpose of Bi_2O_3 addition to the studied $BaTiO_3$ ceramics was to increase its phase and structural homogeneity. The mechanism of the excess positive charge compensation accompanying Bi^{3+} incorporation in A-positions of the perovskite lattice involved binding the available barium vacancies. Because of partial occupation of vacant Ba^{2+} positions by Bi^{3+} and respective charge balancing, the amount of polytitanate secondary phases in the doped $BaTiO_3$ ceramics was significantly lowered compared to the pure ceramics.

Decreased concentration of charged defects upon the incorporation of Bi^{3+} ions in the barium positions in $BaTiO_3$ ceramics caused a reduced sensitivity of the dielectric constant to frequency and lowered the values of the loss tangent. Besides, the excess positive charge of bismuth ions in the A-positions contributed to higher polarization of the Ti^{4+} ion and to enhanced ferroelectric properties of the material [25]. The values of the dielectric constant calculated at different temperatures indicated the diffused nature of the ferroelectric phase transition in Bi-doped $BaTiO_3$ ceramics.

Room-temperature values of ε and tgδ obtained in this work for Bi-modified $BaTiO_3$ ceramics corresponded well to the data reported earlier [23,25]. The optimum values were observed in the case of $BaTiO_3$ ceramics sintered at 1225 °C with addition of 0.1 or 0.5 mol % Bi_2O_3.

Despite a significant improvement in the phase, structural, and dielectric properties of $BaTiO_3$ ceramics resulting from Bi-doping, no appreciable compaction of the material was achieved. A possible solution to this problem would be to increase the sintering duration up to several hours while maintaining the other processing parameters as specified in the current work. However, Bi_2O_3 proved itself to be an effective additive and modifier for $BaTiO_3$ synthesized in water vapor.

4. Materials and Methods

Barium titanate powder was synthesized from TiO_2 in rutile modification (STP TU KOMP 2-340-11, ≥99.5% purity, Komponent-Reaktiv, Moscow, Russia) and BaO (TU 6-09-03-375-74, ≥98% purity). Starting reagents were mechanically mixed maintaining the molar ratio of Ba/Ti = 1.00; 1.10; 1.20; or 1.25 and subsequently sieved through a nylon sieve (300 μm cell size) three times. The mixture was placed in into a PTFE container inside a stainless-steel autoclave with inner volume of 80 mL. Distilled water in the amount of 21 mL was poured into the autoclave outside the PTFE container. Then, the autoclave was sealed and heated up to 200 °C over 1 h. The corresponding autogenous vapor pressure inside the reactor reached 1.55 MPa. The reaction mixture was held under these conditions for 16 h. After that, the autoclave was rapidly cooled down to room temperature so that the vapor inside it condensed mainly at the bottom, separately from the product. The resulting powder was removed from the opened reactor and washed with a large amount of dilute acetic acid and then distilled water until neutral pH of the solution. The powder was filtered and dried in air at 60–70 °C for 12 h.

Portions of the synthesized $BaTiO_3$ powder were mixed with the calculated amounts of Bi_2O_3 (VTU 1-48, 99% purity; mean particle size of 10.5 μm, UZHP, Verkhnyaya Pyshma, Russia) in isopropanol medium with the use of planetary ball mill over 30 min at a rate of 300 min^{-1}. Addition of Bi_2O_3 amounted to 0.1, 0.5, 2.5, and 5.0 mol % of Bi-ions of their total quantity with Ba-ions in the $BaTiO_3$ sample. After the milling procedure, the obtained mixtures were dried in air at 70 °C for 12 h. and sieved subsequently through sieves with 500 and 1000 μm cell size. To prepare the press-powders, 5 wt % of paraffin was added as a temporary technological binder to each of the samples. The procedure of the binder addition included the steps of paraffin melting, its dilution with ethyl acetate, and addition of the powder to the solution. The obtained slurry was continuously mixed while heating until all the ethyl acetate evaporated. The dry powders covered with paraffin were sieved through a sieve of 500 μm cell size. The prepared press-powders were compacted uniaxially at 100 MPa at room temperature and sintered at 1200, 1225, or 1250 °C in air over 1 h. The sequence of ceramic processing operations is presented schematically in Figure 10.

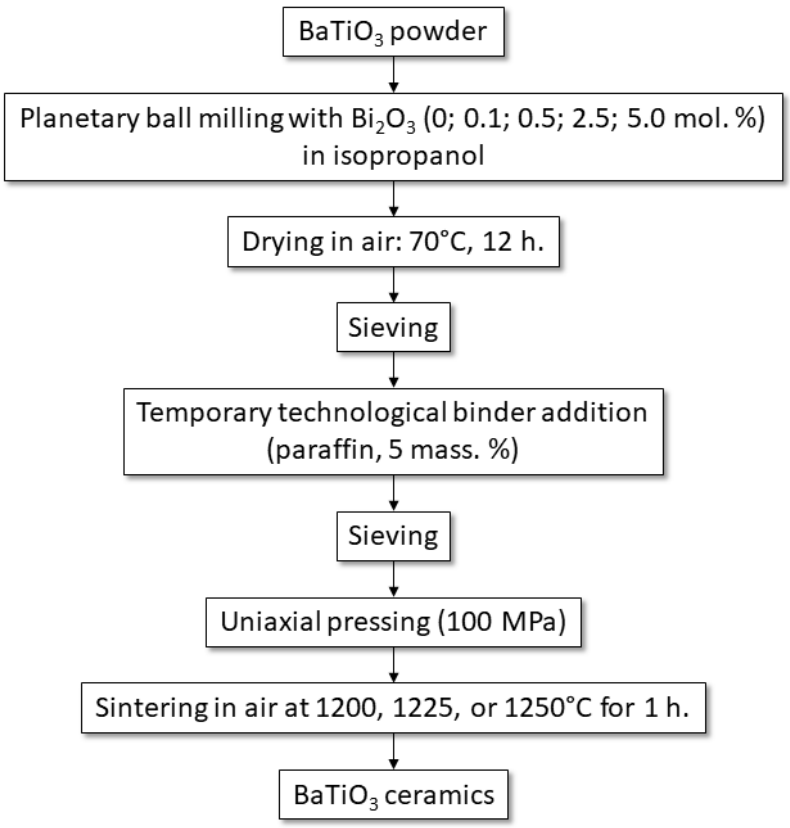

Figure 10. $BaTiO_3$ ceramic processing scheme.

JEOL JSM 6390 LA scanning electron microscope (JEOL Ltd., Tokyo, Japan) was used for investigation of synthesized $BaTiO_3$ powder morphology and microstructure of the manufactured ceramics, as well as for energy dispersive X-ray analysis (EDX) of the ceramics.

X-ray diffraction (XRD) patterns of powder and ceramic samples were registered at Rigaku D/Max-2500 diffractometer (Rigaku Corporation, Tokyo, Japan) with Cu Kα radiation in a range of $10° \leq 2\theta \leq 70°$ with a step of 0.02°. Phase contents of the samples were determined by comparison of the experimental patterns with the data of PDF-2 database. GSAS program package [45] was applied for fitting of the diffraction pattern profiles by the Le Bail method and for Rietveld refinement of the unit cell.

X-ray fluorescent (XRF) analysis of $BaTiO_3$ samples was performed at ARL 9900 Workstation spectrometer (Thermo Fisher Scientific Inc., Waltham, MA, USA). The measured data were processed by the fundamental parameters method.

The apparent density of ceramics was estimated by the Archimedes method. The procedure included the following steps. First, dry ceramic samples were weighed (m_1—weight of a dry sample). Then, they were weighed dipped in kerosene (m_2—weight in liquid) and retrieved therefrom (m_3—weight of a sample saturated with liquid). The apparent density was calculated using Equation (1):

$$\rho = \frac{m_1}{m_3 - m_2}\,\rho_k \quad (1)$$

where ρ_k is the density of kerosene at the corresponding temperature.

The compression strength of ceramic samples was measured by means of an electromechanical testing machine LFM-C (Walter + Bai AG, Löhningen, Switzerland).

The dielectric properties of the manufactured ceramics were studied with the use of a precision LCR meter Agilent E 4980A (Agilent Technologies, Inc., Santa Clara, CA, USA). The bases of the disc-shaped ceramic samples were polished and painted with silver paste. Then the samples were heated up to 800 °C for 20 min. for metallization. Capacitance measurements were conducted in a frequency range of 20 Hz to 2 MHz at a temperature range of 25 to 150 °C.

5. Conclusions

The present work achieved an effect of Bi_2O_3 addition on the properties of ceramics produced from Ba-deficient $BaTiO_3$ powder synthesized in water vapor conditions. Addition of Bi^{3+} ions in amounts within the limit of its solubility in $BaTiO_3$ resulted in an improvement of the phase, structural, and dielectric properties of the ceramic material. Occupation of vacant Ba^{2+} positions by Bi^{3+} ions suppressed formation of polytitanate secondary phases during the sintering. Higher phase homogeneity achieved owing to Bi-doping manifested itself in the uniformity of the ceramic microstructure compared to previous results on sintering of non-doped $BaTiO_3$ ceramics based on this type of initial powder. Incorporation of Bi^{3+} ions into the $BaTiO_3$ ceramic structure led to relative stabilization of its dielectric properties (dielectric constant and loss tangent) in a range of 20 Hz to 2 MHz at room temperature. Doping with Bi^{3+} caused a slight shift of the $BaTiO_3$ ferroelectric phase transition towards higher temperature as well as lowering of the dielectric constant maximum. The revealed effects defined Bi_2O_3 as a perspective additive for production of functional ferroelectric ceramics from $BaTiO_3$ powder synthesized in water vapor.

Author Contributions: Conceptualization, M.D. and V.K.; methodology, Y.I., A.S., and A.F.; validation, A.K., A.S., Y.I., and A.F.; formal analysis, A.K., A.S., and Y.I.; investigation, A.K., A.S., Y.I., G.M., and A.F. ; resources, Y.I., A.S., and V.K.; data curation, A.K., A.S., and A.F.; writing—original draft preparation, A.K., A.S., and S.P.; writing—review and editing, A.K.; visualization, A.K. and Y.I.; supervision, M.D. and V.K.; project administration, M.D.; funding acquisition, M.D. All authors have read and agreed to the published version of the manuscript.

Funding: The work was carried out with the financial support of The Ministry of Education and Science of the Russian Federation within the framework of the State Task "The Development of a Perspective Method for Obtaining of Ultra Dispersive Barium Titanate ($BaTiO_3$) as a Main Component in the Production of Ceramic Capacitors" No. 0699-2017-0005 from 31 May 2017 and with the use of equipment of the Centre of Collective Usage "High Technology in Engineering" of Moscow Polytech (Number for publications: 0699-2017-0005).

Acknowledgments: The work was supported in part by M.V. Lomonosov Moscow State University Program of Development.

Conflicts of Interest: The authors declare no conflict of interest.

References

1. Bhalla, A.S.; Guo, R.; Roy, R. The perovskite structure—A review of its role in ceramic science and technology. *Mater. Res. Innov.* **2000**, *4*, 3–26. doi:10.1007/s100190000062.
2. Eshita, T.; Tamura, T.; Arimoto, Y. Ferroelectric random access memory (FRAM) devices. In *Advances Non-Volatile Memory Storage Technol*; Nishi, Y., Ed.; Woodhead Publishing: Sawston, UK, 2014; pp. 434–454. doi:10.1533/9780857098092.3.434.
3. Saravanan, R. *Titanate Based Ceramic Dielectric Materials*; Materials Research Forum LLC: Millersville, PA, USA, 2018. doi:10.21741/9781945291555.
4. Gao, J.; Xue, D.; Liu, W.; Zhou, C.; Ren, X. Recent Progress on $BaTiO_3$-Based Piezoelectric Ceramics for Actuator Applications. *Actuators.* **2017**, *6*, 24. doi:10.3390/act6030024.

5. Matthias, B.T.; Von Hippel, A. Domain Structure and Dielectric Response of Barium Titanate Single Crystals. *Phys. Rev.* **1948**, *73*, 1378.
6. Chaim, R.; Levin, M.; Shlayer, A.; Estournes, C. Sintering and densification of nanocrystalline ceramic oxide powders: a review. *Adv. Appl. Ceram.* **2008**, *107*, 159–169. doi:10.1179/174367508 × 297812.
7. Somiya, S.; Komarneni, S.; Roy, R. Ceramic Powders for Advanced Ceramics: What are Ideal Ceramic Powders for Advanced Ceramics? *Trans. Mater. Res. Japan.* **2012**, *20*, 47–57. doi:10.14723/tmrsj.35.473.
8. Petzow, G.; Kaysser, W.A. Sintering with additives. *J. Japanese Soc. Powder Metall.* **1987**, *34*, 235–247.
9. Ghyngazov, S.A.; Shevelev, S.A. Effect of additives on sintering of zirconia ceramics. *J. Therm. Anal. Calorim.* **2018**, *134*, 45–49. doi:10.1007/s10973-018-7249-0.
10. Xue, L.A.; Chen, I.-W. Low-Temperature Sintering of Alumina with Liquid-Forming Additives. *J. Am. Ceram. Soc.* **1991**, *74*, 2011–2013.
11. Kholodkova, A.; Danchevskaya, M.; Fionov, A. Study of Nanocrystalline Barium Titanate Formation in Water Vapour Condition. In Proceedings of International Conference NANOCON 2012, Brno, Czech Republic, EU, 23–25 October 2012; Tanger Ltd.: Ostrava, Czech Republic, 2012; pp. 3–8.
12. Kholodkova, A.; Danchevskaya, M.; Popova, N.; Pavlyukova, L.; Fionov, A. Preparation and dielectric properties of thermo-vaporous $BaTiO_3$ ceramics. *Mater. Tehnol*. **2015**, *49*, 447–451. doi:10.17222/mit.2013.276.
13. Kholodkova, A.A.; Danchevskaya, M.N.; Ivakin, Y.D.; Muravieva, G.P.; Tyablikov A.S. Crystalline barium titanate synthesized in sub- and supercritical water. *J. Supercrit. Fluids.* **2016**, *117*, 194–202. doi:10.1016/j.supflu.2016.06.018.
14. Kholodkova, A.A.; Danchevskaya, M.N.; Ivakin, Y.D.; Muravieva, G.P. Synthesis of fine-crystalline tetragonal barium titanate in low-density water fluid. *J. Supercrit. Fluids*. **2015**, *105*, 201–208. doi:10.1016/j.supflu.2015.05.004.
15. Kholodkova, A.A.; Danchevskaya, M.N.; Ivakin, Y.D.; Muravieva, G.P.; Ponomarev, S.G. Effect of Reagents on the Properties of Barium Titanate Synthesized in Subcritical Water. *Russ. J. Phys. Chem. B.* **2018**, *12*, 1261–1268. doi:10.1134/S1990793118080079.
16. Acosta, M.; Novak, N.; Rojas, V.; Patel, S.; Vaish, R.; Koruza, J.; Rossetti, G.A.; Rödel, J. $BaTiO_3$-based piezoelectrics: Fundamentals, current status, and perspectives. *Appl. Phys. Rev.* **2017**, *4*, 041305. doi:10.1063/1.4990046.
17. Haertling, G.H. Ferroelectric Ceramics: History and Technology. *J. Am. Ceram. Soc.* **1999**, *82*, 797–818. doi:10.1111/j.1151-2916.1999.tb01840.x.
18. Wu, S.; Wei, X.; Wang, X.; Yang, H.; Gao, S. Effect of Bi_2O_3 Additive on the Microstructure and Dielectric Properties of $BaTiO_3$-Based Ceramics Sintered at Lower Temperature. *J. Mater. Sci. Technol.* **2010**, *26*, 472–476. doi:10.1016/S1005-0302(10)60075-8.
19. Vittayakorn, W.C.; Banjong, D.; Vittayakorn, N. Processing and Characterization of Bi_2O_3/$BaTiO_3$ Ceramic. *Adv. Mater. Res.* **2013**, *802*, 7–11. doi:10.4028/www.scientific.net/AMR.802.7.
20. Mahapatra, A.; Parida, S.; Sarangi, S.; Badapanda, T. Dielectric and Ferroelectric Behavior of Bismuth-Doped Barium Titanate Ceramic Prepared by Microwave Sintering. *JOM* **2015**, *67*, 1896–1904. doi:10.1007/s11837-014-1266-7.
21. Nath, A.K.; Medhi, N. Piezoelectric properties of environmental friendly bismuth doped barium titanate ceramics. *Mater. Lett*. **2012**, *73*, 75–77. doi:10.1016/j.matlet.2011.12.113.
22. Sadeghzadeh Attar, A.; Salehi Sichani, E.; Sharafi, S. Structural and dielectric properties of Bi-doped barium strontium titanate nanopowders synthesized by sol-gel method. *J. Mater. Res. Technol.* **2017**, *6*, 108–115. doi:10.1016/j.jmrt.2016.05.001.
23. Maurya, D.; Priya, S. Effect of Bismuth Doping on the Dielectric and Piezoelectric Properties of $Ba_{1-x}Bi_xTiO_3$ Lead-Free Ceramics. *Integr. Ferroelectr.* **2015**, *166*, 186–196. doi:10.1080/10584587.2015.1092629.
24. Wang, J.; Rong, G.; Li, N.; Li, C.; Jiang, Q.; Cheng, H. Dielectric Properties of Bi-Doped $BaTiO_3$-Based Ceramics Synthesized by Liquid-State Method. *Russian J. Appl. Chem.* **2015**, *88*, 533–537. doi:10.1134/S107042721503026X.
25. Sareecha, N.; Shah, W.A.; Mirza, M.L.; Maqsood, A.; Awan, M.S. Electrical investigations of Bi-doped $BaTiO_3$ ceramics as a function of temperature. *Phys. B Phys. Condens. Matter.* **2018**, *530*, 283–289. doi:10.1016/j.physb.2017.11.069.
26. Zhou, L.; Vilarinho, P.M.; Baptista, J.L. Relaxor behavior of $(Sr_{0.8}Ba_{0.2})TiO_3$ ceramic solid solution doped with bismuth. *J. Electroceramics.* **2000**, *5*, 191–199. doi:10.1023/A:1026586226361.

27. Badapanda, T.; Senthil, V.; Rana, D.K.; Panigrahi, S.; Anwar, S. Relaxor ferroelectric behavior of "A" site deficient Bismuth doped Barium Titanate ceramic. *J. Electroceramics*. **2012**, *29*, 117–124. doi:10.1007/s10832-012-9754-z.
28. Zhou, L.; Vilarinho, P.M.; Baptista, J.L. Solubility of bismuth oxide in barium titanate. *J. Am. Ceram. Soc.* **1999**, *82*, 1064–1066. doi:10.1111/j.1151-2916.1999.tb01875.x.
29. Nair, K.M.; Bhalla, A.S.; Hirano, S.-I.; Suvorov, D.; Schwartz, R.W.; Zhu, W. *Ceramic Materials and Multilayer Electronic Devices*; John Wiley & Sons, Inc.: Hoboken, NJ, USA, 2012.
30. Beuerlein, M.A.; Kumar, N.; Usher, T.M.; Brown-Shaklee, H.J.; Raengthon, N.; Reaney, I.M.; Cann, D.P.; Jones, J.L.; Brennecka, G.L. Current Understanding of Structure–Processing–Property Relationships in $BaTiO_3$–$Bi(M)O_3$ Dielectrics. *J. Am. Ceram. Soc*. **2016**, *99*, 2849–2870. doi:10.1111/jace.14472.
31. Padmini, P.; Kutty, T.R.N. Influence of Bi^{3+} ions in enhancing the magnitude of Positive Coefficient of Resistance in *n*-$BaTiO_3$ Ceramics. *J. Mater. Sci. Mater. Electron*. **1994**, *5*, 203–209. doi:10.1007/BF00186186
32. Vivekanandan, R.; Kutty, T.R.N. Characterization of barium titanate fine powders formed from hydrothermal crystallization. *Powder Technol.* **1989**, *57*, 181–192. doi:10.1016/0032-5910(89)80074-9.
33. Chen, C.; Wei, Y.; Jiao, X.; Chen, D. Hydrothermal synthesis of $BaTiO_3$: Crystal phase and the Ba^{2+} ions leaching behavior in aqueous medium. *Mater. Chem. Phys.* **2008**, *110*, 186–191. doi:10.1016/j.matchemphys.2008.01.031.
34. Lu, W.; Quilitz, M.; Schmidt, H. Nanoscaled $BaTiO_3$ powders with a large surface area synthesized by precipitation from aqueous solutions: Preparation, characterization and sintering. *J. Eur. Ceram. Soc.* **2007**, *27*, 3149–3159. doi:10.1016/j.jeurceramsoc.2007.01.002.
35. Woo, K.; Choi, G.J.; Sim, S.J.; Cho, Y.S.; Kim, Y.D. Synthesis and characteristics of near-stoichiometric barium titanate powder by low temperature hydrothermal reaction using titanium tetra(methoxyethoxide). *J. Mater. Sci.* **2000**, *35*, 4539–4548. doi:10.1023/A:1004868621334.
36. Li, M.D.; Tang, X.G.; Zeng, S.M.; Jiang, Y.P.; Liu, Q.X.; Zhang, T.F.; Li, W.H. Oxygen-vacancy-related dielectric relaxation behaviours and impedance spectroscopy of $Bi(Mg_{1/2}Ti_{1/2})O_3$ modified $BaTiO_3$ ferroelectric ceramics. *J. Mater.* **2018**, *4*, 194–201. doi:10.1016/j.jmat.2018.03.001.
37. Li, W.B.; Zhou, D.; Xu, R.; Pang, L.X.; Reaney, I.M. $BaTiO_3$-$Bi(Li_{0.5}Ta_{0.5})O_3$, Lead-Free Ceramics and Multilayers with High Energy Storage Density and Efficiency. *ACS Appl. Energy Mater*. **2018**, *1*, 5016–5023. doi:10.1021/acsaem.8b01001.
38. Yamashita, K.; Kuomoto, K.; Yanagida, H. Analogy Between Mechanical and Dielectric Strength Distributions for $BaTiO_3$ Ceramics. Commun. *Am. Ceram. Soc.* **1984**, *67*, C-31–C-33. doi:10.1111/j.1151-2916.1984.tb09617.x.
39. Kishimoto, A.; Koumoto, K.; Yanagida, H. Mechanical and dielectric failure of $BaTiO_3$ ceramics. *J. Mater. Sci.* **1989**, *24*, 698–702. doi:10.1007/BF01107462.
40. Salvini, V.R.; Pandolfelli, V.C.; Spinelli, D. Mechanical Properties of Porous Ceramics. In *Recent Adv. Porous Ceram*; Al-Naib, U.B., Ed.; IntechOpen, Ltd.: London, UK, 2018; pp. 171–199. doi:10.5772/57353.
41. Ramoska, T.; Banys, J.; Sobiestianskas, R.; Vijatovic-Petrovic, M.; Bobic, J.; Stojanovic, B. Dielectric investigations of La-doped barium titanate. *Process. Appl. Ceram.* **2010**, *4*, 193–198. doi:10.2298/pac1003193r.
42. Darlington, C.N.W.; Cernik, R.J. The ferroelectric phase transition in pure and lightly doped barium titanate. *J. Phys. Condens. Matter.* **1991**, *3*, 4555–4567. doi:10.1088/0953-8984/3/25/005.
43. Gulwade, D.; Gopalan, P. Dielectric properties of A- and B-site doped $BaTiO_3$: Effect of La and Ga. *Phys. B Condens. Matter.* **2009**, *404*, 1799–1805. doi:10.1016/j.physb.2009.02.026.
44. Demartin, M.; Herard, C.; Carry, C.; Lamaitre, J. Dedensification and Anomalous Grain Growth during Sintering of Undoped Barium Titanate. *J. Am. Ceram. Soc.* **1997**, *80*, 1079–1084.
45. Larson, A.C.; Von Dreele, R.B. *General Structure Analysis System (GSAS)*; Los Alamos National Laboratory: New Mexico, NM, USA, 2000.